Radiation of sound from a small loudspeaker located in a circular baffle*

Gerald C. Lauchle

Applied Research Laboratory, The Pennsylvania State University, University Park, Pennsylvania 16802
(Received 12 October 1974; revised 15 November 1974)

The exact theory for the radiation of a small loudspeaker in the surface of a rigid circular disk of elliptic profile is presented. Numerical results are included for a monopole at the center of the disk and on its surface. The solution for the loudspeaker in the center of a free circular baffle is then formulated by superimposing the solution of a positive source on one side of the baffle with that for a negative source on the other side. For wavelengths greater than the circumference of the baffle, the resulting field turns out to be very similar to that of a dipole of finite dipole axis. However, for wavelengths smaller than the diameter of the baffle, the diffraction field is shown to be dominated by edge effects. In particular, the total field may also be represented by a simple ring–point source combination, i.e., the edge of the baffle is essentially replaced by a ring source. It is shown that in the vicinity of the axis of the baffle, the shape of the frequency response curve depends little on how much volume flow is generated on the opposite side of the baffle. In other words, it makes little difference (except in absolute level) whether a loudspeaker is enclosed in a box or is permitted to radiate from the rear.

Subject Classification: 20.15, 20.30, 20.55; 85.60.

INTRODUCTION

In this paper the radiation of sound from a loudspeaker located in a rigid finite circular baffle is investigated analytically. The exact solutions arising from the separation of variables of the Helmholtz equation in oblate spheroidal coordinates are used to formulate the bounded Green's function solution of a simple source in the presence of a rigid oblate spheroid. The oblate spheroid is particularly suited to the study of circular disks and pistons because in one limit these shapes are approached. The mathematical developments of oblate spheroidal wave functions are relatively well known and may be found in Bouwkamp,[1] Stratton *et al.*,[2] Leitner and Spence,[3] Meixner and Schäfke,[4] or Flammer,[5] and extensive sets of tables have been compiled by Hanish *et al.*[6]

The sound radiation from oblate spheroids has been treated analytically by Silbiger,[7] and the diffraction of plane waves by oblate spheroids was investigated independently by Spence,[8] Leitner,[9] and Wiener.[10] The radiation field due to a vibrating cap on an oblate spheroid was computed by Nimura and Watanabe,[11] and these results were extended to cover wider ranges of baffle size, curvature, and frequency by Baier.[12]

Of particular interest in this paper is the diffraction field generated by a loudspeaker at the center of a thin circular baffle. The results of the bounded Green's function solution will be used to formulate the loudspeaker solution through use of the superposition principle. The field of a positive source on one side of the baffle is combined with the field of a negative source on the other side. The effective sound generator at the center of the disk is analogous to a very small rigid piston (a loudspeaker) that oscillates with constant velocity amplitude. The total field of this situation is computed and compared to simple sound radiators, such as the dipole and ring source. These comparisons lead to an explanation of the puzzling observation that the shape of the frequency response curve along the axis of the loudspeaker in a box or baffle is practically independent of what occurs on the other side. It makes little difference whether volume flow is occurring on one side or on both, i.e., whether the loudspeaker is open in the back or is enclosed in a box.

It will be assumed throughout that the observation point is far from the baffle and that the harmonic time dependence is $e^{-i\omega t}$, where ω is the circular frequency. The notations used for the spheroidal wave functions follow those of Flammer.[5] The reduced frequencies used in the numerical computations are representative of wavelengths approximately equal to the dimensions of the baffle. This range therefore includes the frequencies for which diffraction effects first appear.

I. OBLATE SPHEROIDAL COORDINATES

The oblate spheroidal coordinates (ξ, η, ϕ) are shown in Fig. 1, and are related to the Cartesian coordinates (x, y, z) by

$$x=\frac{d}{2}[(1-\eta^2)(1+\xi^2)]^{1/2}\cos\phi\,,$$

$$y=\frac{d}{2}[(1-\eta^2)(1+\xi^2)]^{1/2}\sin\phi\,, \tag{1}$$

$$z=\frac{d}{2}\eta\xi\,,$$

where d is the interfocal distance of the generating ellipse. The radial coordinate ξ may range from 0, for an infinitely thin circular piston, to ∞, for a sphere of infinite radius. The diameter of an oblate spheroid $\xi=\xi_0$, is

$$L=d(\xi_0^2+1)^{1/2}\,, \tag{2}$$

and its maximum thickness (at the center) is given by

$$D=\xi_0 d\,. \tag{3}$$

The coordinate η is the angle coordinate and ranges from -1 to $+1$. When equal to $+1$, the positive z axis

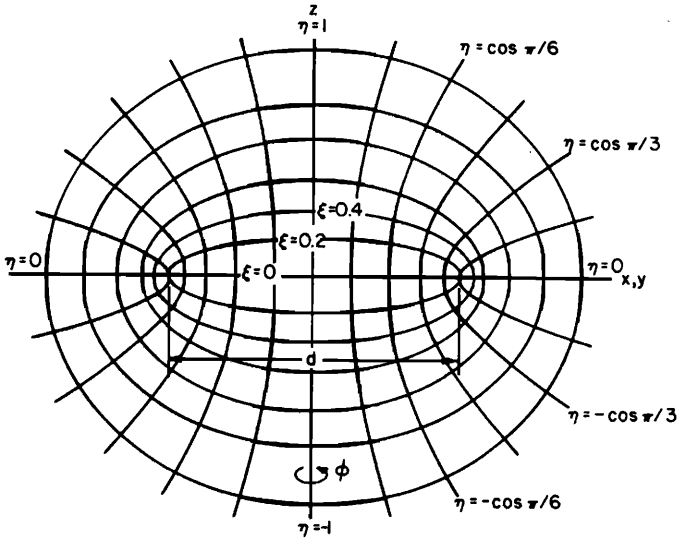

FIG. 1. The oblate spheroidal coordinate system.

(axis of symmetry) is referred to, and $\eta=-1$ is the negative z axis. For $\eta=0$, $z=0$, and the value represents the edge of the disk. The rotational coordinate about the z axis is ϕ, and is identical to the spherical coordinate ϕ.

In the farfield, ξ is large and can be related to the field radius of spherical coordinates:

$$r=\xi d/2\ ,\quad \xi\to\infty\ . \tag{4}$$

In this limit, η, which represents the surface of a hyperboloid, is given by

$$\eta=\cos\theta\ , \tag{5}$$

where θ is the angle between the positive z axis and the asymptote of the hyperboloid. The angle θ is therefore analogous to the spherical aspect angle.

The general modal solution to the wave equation corresponding to harmonic outgoing waves is given by

$$\psi_{mn}=S_{mn}(-ih,\eta)R^{(3)}_{mn}(-ih,i\xi)\cos m\phi\ e^{-i\omega t}\ , \tag{6}$$

where $h=\omega d/2c=kd/2$ (c = sound velocity). The spheroidal angle functions, $S_{mn}(-ih,\eta)$, are orthogonal over the range of η and have the normalization integral (norm) $N_{mn}(h)$. The radial function $R^{(3)}_{mn}(-ih,i\xi)$ represents a diverging wave and is therefore related to the standing wave functions by

$$R^{(3)}_{mn}(i\xi)=R^{(1)}_{mn}(i\xi)+iR^{(2)}_{mn}(i\xi)\ . \tag{7}$$

Here, and in the sequel, the $-ih$ will be dropped from the arguments of the spheroidal functions and the harmonic time dependence will be suppressed. The reader is referred to Flammer[5] for a very complete description of the oblate spheroidal wave functions.

II. ANALYSIS

The problem considered is the general interaction of a spherical acoustic wave with a rigid oblate spheroid. The incident sound field is expressible in terms of the free-space Green's function in oblate spheroidal coordinates.[3,5] The incident acoustic pressure at (ξ,η,ϕ) due to a simple source at (ξ',η',ϕ') is

$$p_i(\xi,\eta,\phi/\xi',\eta',\phi')=\frac{k^2\rho cQ}{2\pi}\sum_{m=0}^{\infty}\epsilon_m\sum_{n=m}^{\infty}\frac{S_{mn}(\eta)S_{mn}(\eta')}{N_{mn}}\cdot\begin{cases}R^{(1)}_{mn}(i\xi)R^{(3)}_{mn}(i\xi'), & \xi<\xi',\\ R^{(1)}_{mn}(i\xi')R^{(3)}_{mn}(i\xi), & \xi>\xi',\end{cases}\cos m(\phi-\phi') \tag{8}$$

where Q is the volume flow of the source, k the wavenumber, ρ the fluid mass density of the medium, and $\epsilon_0=1$, $\epsilon_m=2(m>0)$. By assuming the diffracted pressure to be a series of spheroidal harmonics given by the form of Eq. 6, i.e.,

$$p_d(\xi,\eta,\phi)=\sum_{m=0}^{\infty}\sum_{n=m}^{\infty}A_{mn}S_{mn}(\eta)R^{(3)}_{mn}(i\xi)\cos m\phi\ , \tag{9}$$

and applying the boundary condition

$$\left[\frac{\partial(p_i+p_d)}{\partial\xi}\right]_{\xi=\xi_0}=0\ , \tag{10}$$

where ξ_0 is the boundary of the given spheroidal body, results in

$$p_b(\xi,\eta,\phi)=-\frac{k^2\rho cQ}{2\pi}\sum_{m=0}^{\infty}\epsilon_m\sum_{n=m}^{\infty}\frac{S_{mn}(\eta)S_{mn}(\eta')}{N_{mn}}\cos m(\phi-\phi')\cdot\left[R^{(3)}_{mn}(i\xi')R^{(3)}_{mn}(i\xi)\frac{R^{(1)\prime}_{mn}(i\xi_0)}{R^{(3)\prime}_{mn}(i\xi_0)}-\begin{cases}R^{(1)}_{mn}(i\xi)R^{(3)}_{mn}(i\xi'), & \xi<\xi',\\ R^{(1)}_{mn}(i\xi')R^{(3)}_{mn}(i\xi), & \xi>\xi',\end{cases}\right] \tag{11}$$

where the prime on the radial functions denotes differentiation with respect to ξ, and $p_b=p_i+p_d$.

III. MONOPOLE AT THE CENTER

In this section, the special case of a monopole situated at the center and on the surface of a thin ($L/D\gg1$) oblate spheroid is considered. The solution no longer depends on ϕ (axisymmetric), so only the $m=0$ terms need be retained. Assuming that the sound source is located at $\xi'=\xi_0$, $\eta'=-1$, and replacing $R^{(3)}_{mn}(i\xi)$ with its asymptotic value for $\xi\to\infty$, i.e.,

$$R^{(3)}_{mn}(i\xi)\underset{\xi\to\infty}{\longrightarrow}(h\xi)^{-1}\exp[ih\xi-i\pi(n+1)/2]\ , \tag{12}$$

results in the farfield solution. It is expedient to normalize with the sound field generated by the sound source in the absence of the baffle,

$$p_s=-\frac{ik\rho cQ}{4\pi r}\,e^{ikr}\ . \tag{13}$$

The resulting expression for the normalized pressure field is then of the form:

$$\frac{p_b}{p_s}=\frac{-2}{h(\xi_0^2+1)}\sum_{n=0}^{\infty}(-i)^{n+1}\frac{S_{0n}(\eta)S_{0n}(-1)}{N_{0n}R^{(3)\prime}_{0n}(i\xi_0)}\ , \tag{14}$$

where the Wronskian relation[5] $W[R^{(1)}_{mn},R^{(2)}_{mn}]=1/[h(\xi_0^2+1)]$ was used. From the definition of h and from Eq. 4, we let $h\xi=kr$ in the derivation of Eq. 14.

Numerical evaluations of the partial wave series of Eq. 14 were performed using the IBM 360/67 digital computer located on The Pennsylvania State University Campus. A value of 0.02 for ξ_0 was selected to be rep-

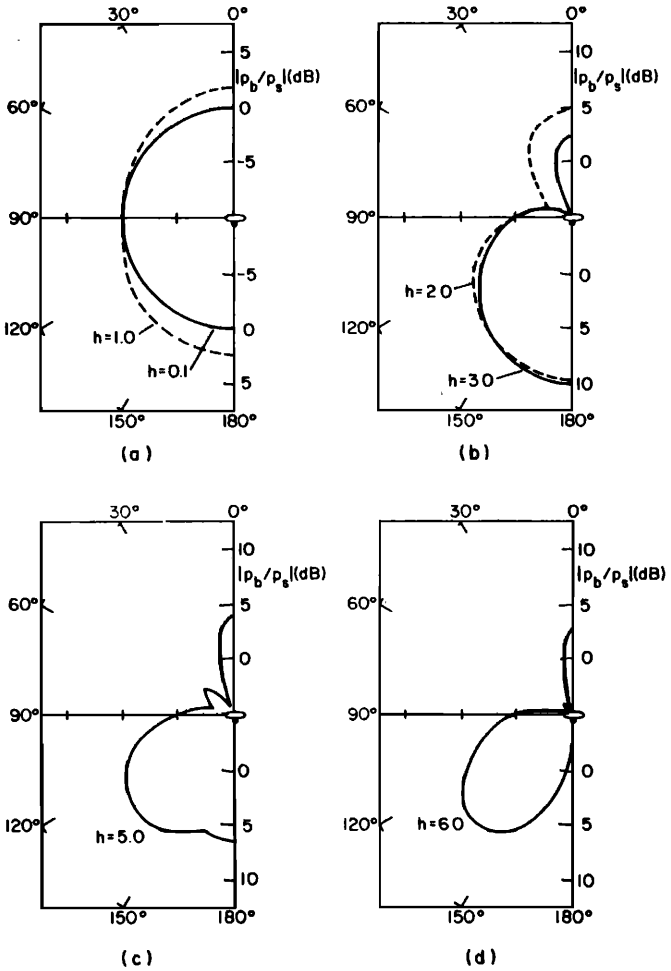

FIG. 2. Computed directivity curves for a single source at the center and on the surface of a rigid oblate spheroidal baffle ($\xi_0 = 0.02$). The source is situated on the 180° axis. (a) Patterns for $h = 0.1$ and 1.0. (b) Patterns for $h = 2.0$ and 3.0. (c) Pattern for $h = 5.0$. (d) Pattern for $h = 6.0$.

resentative of a thin baffle ($L/D = 50$). The radial functions required for the computations were taken from the tables of Hanish *et al.*,[6] and the angle functions were computed from their exact series expansion of Legendre polynomials. The expansion coefficients, required for the generation of spheroidal functions, were computed with the aid of a program developed by Hodge.[13] The normalization integral was obtained by numerically integrating the square of the angle function over the range of η.

Figures 2 and 3 show the results of these computations in the form of directivity curves for several values of the reduced frequency h. The largest value of h considered was 9.0, for which it was found that the series converged in approximately ten terms. This observation is not surprising because spheroidal radial functions of the first kind behave in a manner similar to Bessel functions as the degree increases above the value of the argument. These curves show the modulus (in decibels) of Eq. 14 as a function of $\theta = \cos^{-1}\eta$ with the monopole location indicated by the small dot at $\theta = 180°$.

When $h \leq 1$, or more precisely when $\lambda > \pi d$ (λ = acoustic wavelength), the patterns are basically omnidirectional, i.e., the baffle has little effect on the field of the source. As the frequency variable increases, lobes begin to appear because of the diffraction effects caused by the baffle. When $h = 3.0$, or when the wavelength approximately equals the diameter of the baffle, a strong minimum occurs near the 30° direction. If one looks at the diffracted wave in the x–z plane in terms of a ray, it is easy to see that in the 30° direction, that part of the wave leaving the edge at 270° lags that contribution from the 90° edge by the phase angle π. The resultant pressure, therefore, approaches zero.

A result which may seem strange at first glance is the pattern for $h = 6.0$, where the wavelength approximately equals the radius of the baffle. A minimum occurs along the axis of the baffle on the side of the source. The diffraction wave generated in the plane of the baffle then has the same phase as the incident wave at the edges. The abrupt change of curvature at the edges (radius of curvature at the edge equals $D^2/4L$) and the availability of the full space for the outcoming wave then creates a situation similar to the propagation of a wave in an open-end duct. The wave reflects from the medium at the edges in antiphase, relative to the source point. The acoustic pressure in the 180° direction due to the incident wave is proportional to Qe^{ikr} and that diffracted from the edge is proportional to $Qe^{i(kr+\pi)}$. The resultant of these two fields is seen to be very small.

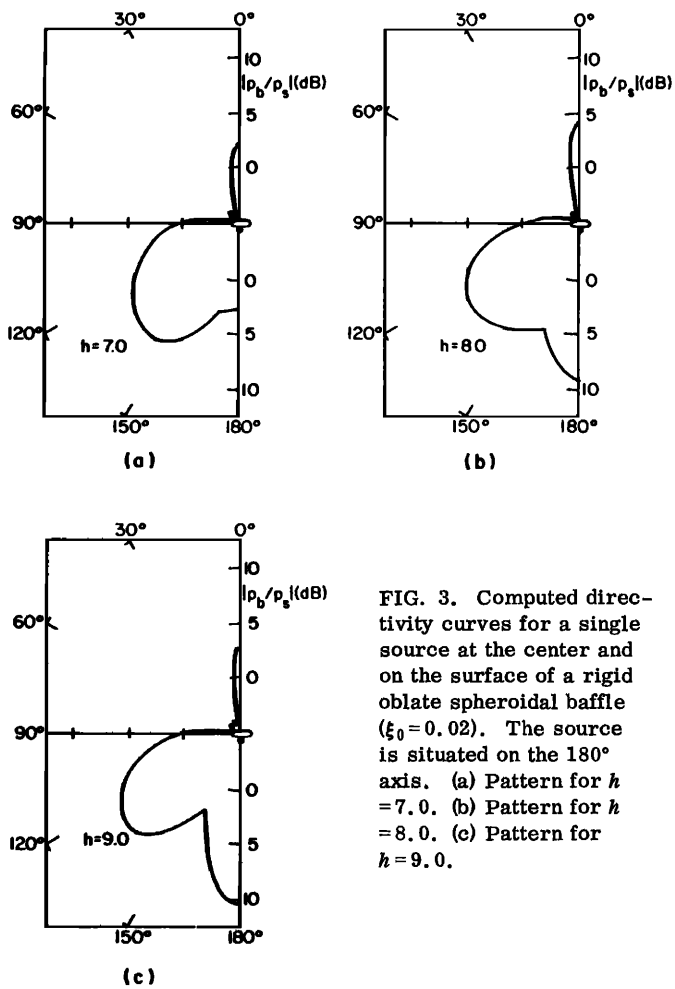

FIG. 3. Computed directivity curves for a single source at the center and on the surface of a rigid oblate spheroidal baffle ($\xi_0 = 0.02$). The source is situated on the 180° axis. (a) Pattern for $h = 7.0$. (b) Pattern for $h = 8.0$. (c) Pattern for $h = 9.0$.

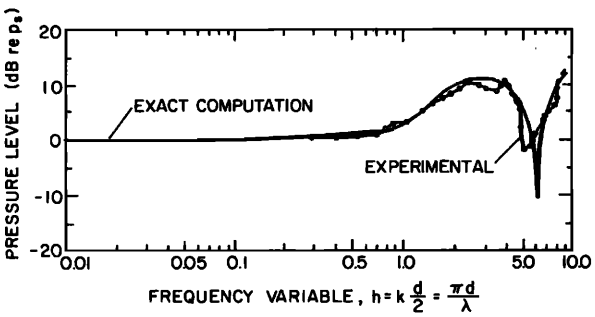

FIG. 4. The on-axis frequency response on the side of the baffle in which the single sound source is located (the experimental curve is due to Wiener[10]).

Note that a strong beam (Poisson spot) occurs at all wavelengths along the path opposite the sound source ($\theta = 0°$). This result is expected since the phase shift is zero between the edges of the disk along this path, and constructive interference occurs.

The farfield pressure ratio in the 180° direction is presented as a function of h in Fig. 4. Wiener[10] has measured the pressure on the surface of a circular disk when insonified by a plane wave. The principle of reciprocity allows us to interpret those results as the farfield pressure due to a sound source on the surface. The particular experimental curve of Wiener for axial incidence and the pressure at the center on the lit side is shown along with the computed curve in Fig. 4. The agreement is seen to be good with only a slight discrepancy at the minimum. The peak is seen to occur for $h \approx \pi$, or when the wavelength equals the diameter of the baffle. The result supports the same arguments presented for $h \approx 2\pi$, except that in this case the diffracted edge wave is in phase with the incident wave and the two combine constructively.

IV. LOUDSPEAKER AT THE CENTER

At low frequencies, a loudspeaker may be considered as an oscillating piston source. If such a source were placed at the center of a thin circular disk, the volume flow on the top of the disk would be in antiphase to the volume flow on the bottom surface. With this idea in mind, we can use the results for the point source at the center of an oblate spheroid to formulate an acoustic model that represents a small loudspeaker in a free circular baffle. The procedure is to superimpose the solution of a positive monopole situated at $\eta = 1$ with the solution for a monopole of opposite (negative) strength located at $\eta = -1$.

Equation 14 represents the solution for a single source at $\eta = -1$. Subtracting the pressure field due to a source at $\eta = 1$ from that field due to a source at $\eta = -1$, and noting that

$$S_{0n}(-1) - S_{0n}(1) = -2S_{0n}(1), \quad n \text{ odd},$$
$$= 0, \quad n \text{ even}, \qquad (15)$$

results in

$$\frac{p}{p_s} = \frac{4}{h(\xi_0^2+1)} \sum_{n=1}^{\infty}{}' (-1)^{(n+1)/2} \frac{S_{0n}(\eta) S_{0n}(1)}{N_{0n} R_{0n}^{(3)\prime}(i\xi_0)}, \qquad (16)$$

where the prime on the summation symbol means summation over only even or odd terms depending on the starting value. The quantity (p/p_s) denotes the total pressure field from the double source arrangement normalized with the sound field of a simple source (Eq. 13) in the absence of a baffle.

The total sound field of the loudspeaker in a thin circular baffle ($\xi_0 = 0.02$) has been computed from Eq. 16 using the same numerical procedure discussed in Sec. III. The results for $h \leq 3$ are shown in Fig. 5. The baffle generates very much the same patterns as the two sources at the specified separation distance. The field is basically that of a dipole. Nimura and Watanabe[11] show essentially the same patterns for a finite piston oscillating at the center of an oblate spheroid which supports our hypothesis that this model represents a loudspeaker at low frequencies. Since the patterns appear to be dipole, we may use the results of dipole radiation to predict the exact results. In particular, the normalized amplitude of a dipole is expressible as

$$\left|\frac{p_d}{p_s}\right| = 2\sin\left(\frac{kb}{2}\cos\theta\right) = 2\sin\left(h\frac{b}{d}\cos\theta\right), \qquad (17)$$

where b is the dipole axis. By setting the amplitude of the exact computations equal to the amplitude of the equivalent dipole at $\theta = 0°$ (on-axis) results in the required dipole axis as a function of reduced frequency, i.e.,

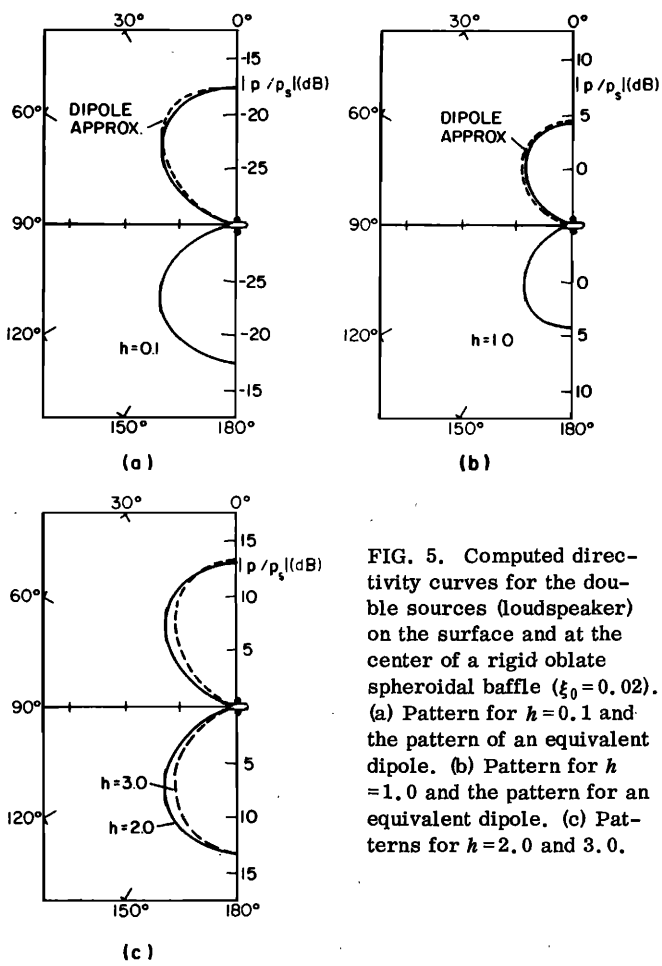

FIG. 5. Computed directivity curves for the double sources (loudspeaker) on the surface and at the center of a rigid oblate spheroidal baffle ($\xi_0 = 0.02$). (a) Pattern for $h = 0.1$ and the pattern of an equivalent dipole. (b) Pattern for $h = 1.0$ and the pattern for an equivalent dipole. (c) Patterns for $h = 2.0$ and 3.0.

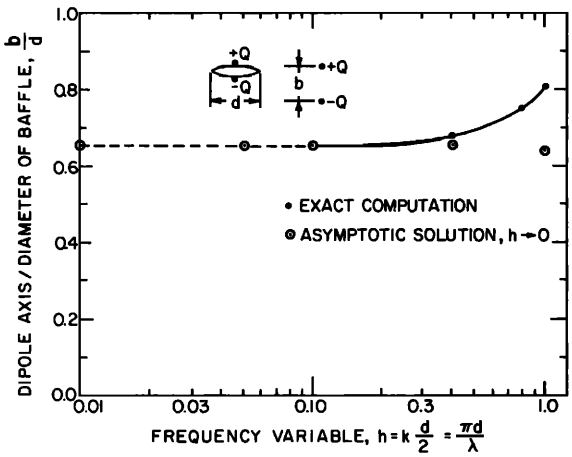

FIG. 6. The equivalent dipole axis as a function of reduced frequency h, for which a dipole may be used to represent the field of a loudspeaker in a free circular baffle.

$$b/d = h^{-1}\sin^{-1}(|p/p_s|/2), \tag{18}$$

where $|p/p_s|$ is the modulus of the exact result at $\theta = 0°$. In using Eq. 18 it was found that the exact values of the pressure ratio fell within a range that makes the arc sine function undefined when $1 \le h \le 3$. The conclusion drawn from this is that the field for $h > 1$ cannot be approximated by a dipole.

The variation of b/d with h is shown in Fig. 6, where these values, when substituted into Eq. 17 result in the broken line patterns of Fig. 5(a) and Fig. 5(b). It is seen that b/d approaches a constant as h tends to zero. This constant is easily deducible from Eq. 16 if the asymptotic values of the spheroidal wave functions for small h are used. Silbiger[7] has presented the appropriate asymptotic formulas for $h \to 0$, and their incorporation into Eq. 16 results in

$$\frac{p}{p_s}\underset{h\to 0}{\longrightarrow} -2ih\cos\theta\left[\frac{\pi\xi_0/2 - \xi_0\tan^{-1}(\xi_0) - 1}{\pi/2 - \xi_0/(\xi_0^2+1) - \tan^{-1}(\xi_0)} - \xi_0\right], \tag{19}$$

where only the first two terms of the series were retained and terms of $0(h^4)$ and smaller were neglected. The angular variation is seen to be $\cos\theta$, which is identical to that of a dipole. Using Eq. 19 in Eq. 18 results in the asymptotic value of b/d, i.e.,

$$b/d \underset{h\to 0}{\longrightarrow} \left|\frac{\pi\xi_0/2 - \xi_0\tan^{-1}(\xi_0) - 1}{\pi/2 - \xi_0/(\xi_0^2+1) - \tan^{-1}(\xi_0)} - \xi_0\right|. \tag{20}$$

It is clearly seen that for $\xi_0 \approx 0$, $b/d \to 2/\pi$. This limit, along with some other points computed from Eq. 20, is shown in Fig. 6. The equivalent dipole axis, at low frequencies, is approximately the diameter of the baffle squared divided by half the circumference.

The directivity functions for $h > 3$ are shown in Fig. 7. Diffraction by the baffle has caused the patterns to deviate from simple dipole radiation. The on-axis frequency response is shown in Fig. 8 along with an experimental curve of a loudspeaker in a free-circular baffle measured by Buchmann.[14] The similarity of this curve to the one for a single source (Fig. 4) is remarkable. The extrema occur at the same values of reduced frequency, and the overall shape of the frequency curves is near-

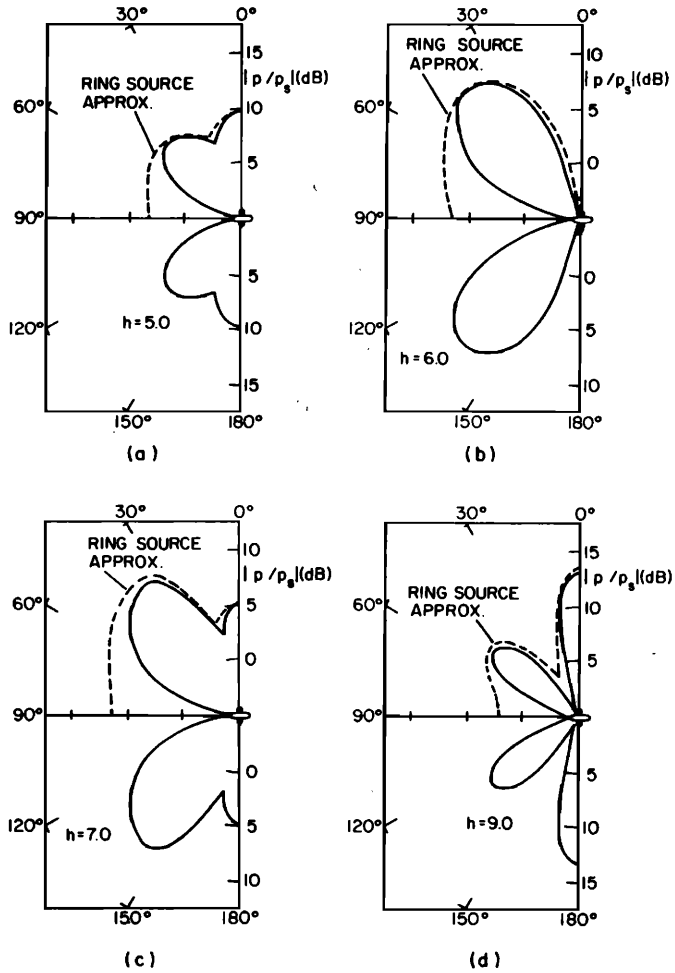

FIG. 7. Computed directivity curves for the double sources (loudspeaker) on the surface and at the center of a rigid oblate spheroidal baffle ($\xi_0 = 0.02$). Included with the exact computations are the patterns of an equivalent ring–point source combination. (a) Patterns for $h = 5.0$. (b) Patterns for $h = 6.0$. (c) Patterns for $h = 7.0$. (d) Patterns for $h = 9.0$.

ly identical. The maximums have occurred at the same frequency because when the loudspeaker has a maximum on the $\eta = -1$ side, the contribution from diffraction by the baffle is in phase with the direct radiation from the point source on that side of the baffle. If the two sources that represent the loudspeaker were in phase (doublet),

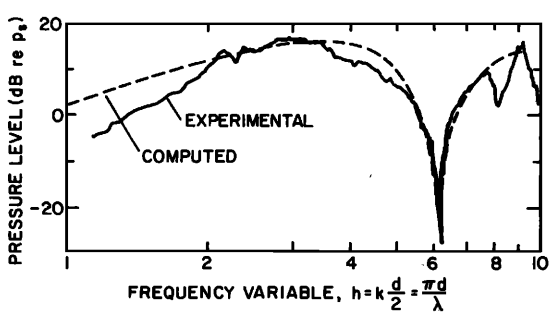

FIG. 8. The on-axis frequency response of the double sources (loudspeaker) in the center of a free circular baffle (the experimental curve is due to Buchmann[14]).

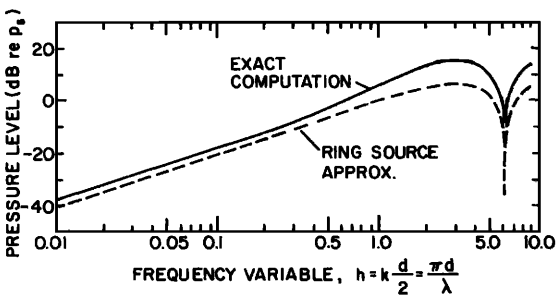

FIG. 9. The on-axis frequency response of the double sources (loudspeaker) in the center of a free circular baffle compared with the result computed by a ring–point source combination.

then too the diffraction field would be in phase and a maximum would occur. Since the single-source solution for a thin baffle may be approximated as one half the sum of the loudspeaker and doublet solutions, then a corresponding maximum would occur in its frequency curve. Conversely, at the frequency for which the loudspeaker solution has a minimum, the diffraction field is 180° out of phase with the direct radiation, and hence, nearly 180° out of phase with the field of the doublet. Their superposition then results in a minimum for the single source situation. The result is that the shape of the frequency response curve depends little on whether there is volume flow on only the front, or on both sides of the baffle; however, the amount of volume flow does affect the absolute pressure levels. Differences of up to 4 dB occur throughout the range from $h = 1$ to $h = 9$.

An often-used technique in scattering problems is to replace the diffraction field by a simple sound radiator whose field corresponds to the given diffraction field. This has been performed for the small h region (dipole approximation) and can also be performed for larger values of h. If edge diffraction is dominant, then the edge of the baffle may be replaced by a simple ring source. It was argued earlier that the reflection of the incident wave from the edge causes a phase shift. An equivalent sound radiator might then be the combination of a ring source with an out-of-phase simple source located at the geometric center of the ring. The field of the simple source of strength $-Q$ and phase angle $kd/2$ is

$$p_{s_1} = \frac{ik\rho cQ}{4\pi r} e^{i(kr + kd/2)}, \tag{21}$$

and the field of a ring source of strength Q and diameter d is, viz., Skudrzyk,[15]

$$p_r = -\frac{ik\rho cQ}{4\pi r} J_0\left(\frac{kd}{2}\sin\theta\right) e^{ikr}. \tag{22}$$

The combination of the two, normalized to p_s is then

$$\frac{(p_r + p_{s_1})}{p_s} = J_0(h\sin\theta) - e^{ih}, \tag{23}$$

where $kd/2$ was replaced by h.

The directivity functions, based on Eq. 23, are plotted as the broken line curves in Fig. 7. The amplitude was shifted by approximately 6 dB, such that the levels are equal along the z axis ($\theta = 0°$). The on-axis frequency response is shown in Fig. 9 without the 6-dB shift. The divergence of the two curves for $h > 1$ is between 6 and 8 dB, meaning a factor of 2 or 2.5, respectively. The factor 2 is expected since, at higher wavenumbers, the wavelength becomes approximately equal to or smaller than the diameter of the baffle. The disk then begins to approach an infinite baffle, and the sound pressure doubles in much the same way as it does for a point source near an infinite plane. This effect is not seen for the ring-source approximation because there is no boundary, and the sound sources radiate into spherical space at all frequencies.

V. CONCLUSIONS

In this paper, the diffraction of sound by a free circular disk of elliptic profile with a monopole or group of monopoles on its surface was treated analytically with the use of spheroidal wave functions. The two specific cases considered were (1) a simple monopole on the surface and located at the center of the disk, and (2) the superposition of a positive monopole on one side of the disk with a negative one located on the other side and both on the axis of symmetry. The latter case depicts a model of a loudspeaker in the center of a circular baffle. For small values of h ($h \leq 1$) the directivity curves of case (1) are monopole and those of case (2) are dipole. The equivalent dipole axis required to reproduce the exact computations was presented. For $h > 1$, the shapes of the on-axis frequency response curves for the two cases were found to be nearly identical. The result indicates that the shape of the frequency curve depends little on whether volume flow is created on only the front side of the baffle, or on both sides. The total field in the vicinity of the axis was then shown to depend primarily on the superposition of the incident sound field and a field due to edge diffraction. This edge diffraction field was approximated by a simple ring source and the comparison to the exact solution was favorable. When applicable, experimental data from other authors were compared with the theoretical computations and agreement was found to be good.

ACKNOWLEDGMENT

The author wishes to thank Professor Eugen J. Skudrzyk for suggesting this problem, and for his assistance in the interpretation of the numerical results. This work was supported by the Applied Research Laboratory under contract with the Naval Sea Systems Command.

*This paper draws from a Ph. D. thesis submitted by the author to the Graduate Faculty of the Engineering Acoustics program at The Pennsylvania State University. This paper was presented at the 85th Meeting of the ASA in Boston, MA on 13 April 1973 [J. Acoust. Soc. Am. 54, 335(A) (1973)].

[1] C. J. Bouwkamp, J. Math. Phys. 26, 79–92 (1947).

[2] J. A. Stratton, P. M. Morse, L. J. Chu, and R. A. Hunter, *Elliptic Cylinder and Spheridal Wave Functions* (Wiley, New York, 1941).

[3] A. Leitner and R. D. Spence, J. Franklin Inst. 249, 299–321 (1950).

[4] J. Meixner and F. W. Schäfke, *Mathieusche Funktionen und*

Späroidfunktionen (Springer–Verlag, Berlin, 1954).
[5]C. Flammer, *Spheroidal Wave Functions* (Stanford U. P., Stanford, CA, 1957).
[6]S. Hanish, R. V. Baier, A. L. Van Buren, and B. J. King, "Tables of Radial Spheroidal Wave Functions," NRL Reps. 7088, 7089, 7091, 7092, and 7093 (June 1970).
[7]A. Silbiger, J. Acoust. Soc. Am. 33, 1515–1522 (1961).
[8]R. D. Spence, J. Acoust. Soc. Am. 20, 380–386 (1948).
[9]A. Leitner, J. Acoust. Soc. Am. 21, 331–334 (1949).
[10]F. M. Wiener, J. Acoust. Soc. Am. 21, 334–347 (1949).
[11]T. Nimura and Y. Watanabe, J. Acoust. Soc. Am. 25, 76–80 (1953).
[12]R. V. Baier, J. Acoust. Soc. Am. 51, 1705–1716 (1972).
[13]D. B. Hodge, "The Calculation of the Spheriodal Wave Equation Eigen Values and Eigen Functions," Ohio State U. Electro Sci. Lab. Rep. No. 3 (1969).
[14]G. Buchmann, Akust. Z. 1, 169–174 (1936).
[15]E. J. Skudrzyk, *The Foundations of Acoustics: Basic Mathematics and Basic Acoustics* (Springer–Verlag, New York and Wien, Austria, 1971).